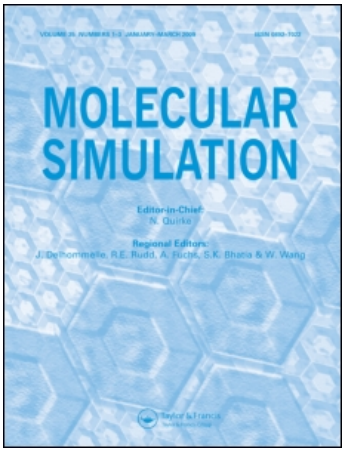

Molecular Simulation
Publication details, including instructions for authors and subscription information:
http://www.informaworld.com/smpp/title~content=t713644482

Density functional study of sulphur hexafluoride (SF_6) and its hydrogen derivatives

Marta Kinga Bruska[a]; Jacek Piechota[b]
[a] Department of Chemistry, Jagiellonian University, Kraków, Poland [b] Interdisciplinary Centre for Materials Modelling, University of Warsaw, Warsaw, Poland

To cite this Article Bruska, Marta Kinga and Piechota, Jacek(2008) 'Density functional study of sulphur hexafluoride (SF_6) and its hydrogen derivatives', Molecular Simulation, 34: 10, 1041 — 1050
To link to this Article: DOI: 10.1080/08927020802258708
URL: http://dx.doi.org/10.1080/08927020802258708

Molecular Simulation
Vol. 34, Nos. 10–15, September–December 2008, 1041–1050

Density functional study of sulphur hexafluoride (SF_6) and its hydrogen derivatives

Marta Kinga Bruska[a] and Jacek Piechota[b]*

[a]*Department of Chemistry, Jagiellonian University, Kraków, Poland;* [b]*Interdisciplinary Centre for Materials Modelling, University of Warsaw, Warsaw, Poland*

(*Received 31 January 2008; final version received 9 June 2008*)

Density functional study has been performed for a group of compounds derived from sulphur hexafluoride (SF_6) by consecutively substituting fluorine with hydrogen. SF_6 is widely used as the insulating gas in the electrical industry and is recognised as one of the greenhouse gases with extraordinary global warming potential. The aim of the present study is to look for potential industrial alternatives to SF_6 as well as to examine mechanisms that can contribute to its faster atmospheric decay. The ground state geometries, binding energies, vibrational spectra, charge distributions, dipole moments, as well as thermodynamic properties for the series of the $SF_{6-n}H_n$ ($n = 0, \ldots, 6$) molecules have been obtained and discussed. For comparison, computational results for the SCl_6 molecule have also been included in the present study.

Keywords: sulphur hexafluoride; greenhouse gases; density functional theory; vibrational analysis

1. Introduction

Interest in the sulphur hexafluoride (SF_6) system stems both from practical and theoretical considerations. It is one of the most popular (next to air) insulating gases, with a breakdown strength of about three times that of air. It has a number of technologically important properties: it is not flammable and non-toxic; at normal temperatures, it is also non-corrosive, and is fairly inert. That is why SF_6 is commonly used in industry as a gaseous dielectric and as a plasma etching gas in applications such as circuit breakers, gas-insulated busbar systems, and also for large-scale scientific applications such as tandem particle accelerators. Other areas of application of SF_6 include the magnesium industry to protect molten magnesium from oxidation and potentially violent burning, and semiconductor manufacturing to create circuitry patterns on silicon wafers. Also, SF_6 is a candidate refrigerant to replace the chlorofluorocarbons (CFCs) that are damaging the ozone layer. For an extensive review of SF_6 technical applications see, for example [1] and publications therein.

Because of its unique structure, unusual spectroscopy and applied interest, the SF_6 molecule has been a subject of much interest both experimentally and theoretically. Photoelectron [2–4], valence-shell [5–7], inner-shell [8–11] photoionisation, valence-shell [12] and inner-shell [13–16] electron energy-loss experimental measurements have been performed. The unique, octahedral symmetry structure of SF_6 provides good example of shape resonance phenomena. The infrared active modes of octahedral molecules are of F_{1u} symmetry and ν_3 as well as ν_4 bands are allowed in absorption [17]. In particular, the region of the ν_3 fundamental near $950\,cm^{-1}$ has very strong absorption. The bond dissociation energy of SF_6 (to $SF_5 + F$) is 3.82 eV, but photodissociation is not observed until the photon energy exceeds ~ 10 eV [18].

On the theoretical side, SF_6 has become a classic molecule for the study of electron attachment at ultralow electron energies. The attachment of low energy electrons to SF_6 results in formation of a metastable negative ion by the process: $SF_6 + e^- \rightarrow SF_6^-$ [18–21]. An understanding of the thermal electron attachment properties and temperature behaviour of rate constant for SF_6 is, in turn, of importance in the design of gaseous insulators and diffuse discharge switchers.

However, at the same time SF_6 is the most potent greenhouse gas that has been evaluated by the Intergovernmental Panel on Climate Change (IPCC), with a global warming potential (GWP) of 22,800 times that of CO_2 when compared over a 100 year period [22]. Two main factors contributing to this extraordinary high value of GWP are strong radiative forcing ($0.52\,Wm^{-2}\,ppb^{-1}$) and a very long atmospheric lifetime (800–3200 years) [22–26]. In the stratosphere, the highest energy solar photons have an energy of ~ 6 eV, so it is very unlikely that SF_6 will be photodissociated there. Therefore, although the concentration of SF_6 is still relatively low in the Earth's atmosphere (5.21 ppt) [26], it is one of the greenhouse gases that the Kyoto Protocol seeks to control [27], as even small amounts of SF_6 emissions can constitute a significant carbon-equivalent emission tonnage.

Apart from destroying the ozone layer, greenhouse gases that can absorb infrared radiation in the so-called

*Corresponding author. Email: jp@icm.edu.pl

ISSN 0892-7022 print/ISSN 1029-0435 online

DOI: 10.1080/08927020802258708
http://www.informaworld.com

'atmospheric window' between the wavelengths of $800-1400\,cm^{-1}$ are of great concern because they are able to trap radiation that would have otherwise been emitted into space. In other words, without greenhouse gases most of the radiation emitted by the Earth's surface at wavelengths within in the atmospheric window would have passed through the Earth's atmosphere without heating it.

Recently, another compound with extremely strong radiative forcing (of $0.59\,Wm^{-2}\,ppb^{1}$), identified as trifluoromethyl sulphur pentafluoride (SF_5CF_3), has been detected in the atmosphere [28,29]. It is supposed that SF_5CF_3 originates as a breakdown product of SF_6 formed by high-voltage discharges in electric industry equipment [28]. Atmospheric lifetime of SF_5CF_3 (~ 800 years) is lower than that of SF_6, but its value of GWP ($\sim 17{,}700$) is one of the highest of all other greenhouse gases [22].

It is worth noting, however, that the greenhouse gases with the greatest GWP values are the fully fluorinated compounds: CF_4, C_2F_6, C_3F_8, *c*-C_4F_8, SF_6, NF_3 and CHF_3, that are widely used by the semiconductor industry [30]. As for now there is no significant mechanism for their destruction in the natural circulation of the Earth's atmosphere – as a result their atmospheric lifetimes are estimated to be up to 50,000 years for CF_4 [22].

In case of CFCs a wide variety of alternative compounds has been investigated with the aim of protecting the ozone layer and reducing the global warming. The basic concept in the process of development of alternative CFCs is the introduction of a hydrogen atom into the CFC molecule to reduce its atmospheric lifetime without detrimenting its properties. In this way, several hydrochlorofluorocarbons and hydrofluorocarbons have already been developed and have found practical use. The introduction of hydrogen atoms into the molecule raises the compound's reactivity towards OH radicals as the reactivity with OH radicals is related to the stability of the molecule in the troposphere [31].

Motivated by this fact we have studied the series of the $SF_{6-n}H_n$ ($n = 0,\ldots,6$) molecules where the fluorine atoms of SF_6 were consecutively replaced with the hydrogen atoms. The aim of the study is to look for potential industrial alternatives to SF_6 as well as to examine mechanisms that can contribute to its faster atmospheric decay. SCl_6 has been also taken into consideration to compare our results with a heavier analogue of the SF_6 molecule. To our best knowledge, this is the first report on the properties of the $SF_{6-n}H_n$ series of compounds.

The present study is based on density functional theory (DFT) [32,33]. This approach has over the past decade emerged as a tangible and versatile computational method with applications in many subfields of chemistry. The DFT-based methods can provide bond energies, structures and other electronic properties of high accuracy. The method has previously been applied to similar studies on diatomic 3*d* transition metal monoxides [34,35].

The rest of the paper is organised as follows. Computational details are reported in Section 2. In Section 3, the ground state geometries, bonding energies, vibrational spectra, charge distributions partitioned by Hirshfeld method, dipole moments, as well as thermodynamic properties are presented and analysed. In Section 4, the main points of this work are summarised and perspectives for future research are outlined.

2. Computational details

As mentioned in the introduction, the computational method used for the purpose of the present study is based on DFT as implemented in the DMol^3 code [36,37] available as part of the Materials Studio® 4.0 software environment (Information available at: http://www.accelrys.com/products/mstudio/). For an extensive review of the DMol^3 description and its features we refer the reader to [36,37] and references therein. We present here only a summary of the input parameters set up in the DMol^3 package in order to get stable and accurate results, as compared to experiment and other calculations.

DMol^3 uses numerical functions on an atom-centred grid as its atomic basis. For the purpose of the present study the DNP basis set was used for all atoms. The DNP basis set uses double-numerical quality basis set with polarisation functions. This means that for each occupied atomic orbital one numerical function is generated and a second set of this functions are given for valence atomic orbitals. It also generates polarisation *d*-functions on all non-hydrogen atoms and polarisation *p*-function on all hydrogen atoms. The DNP basis sets are comparable in quality to Gaussian 6-31G** basis sets.

The quality of the integration grid that controls the selection of mesh points for the numerical integration procedure used in the evaluation of the matrix elements was chosen to be FINE. The electron density in DMol^3 is expanded in terms of multipolar partial densities (auxiliary density) used to specify the maximum angular momentum L_{max} of the multipolar fitting functions that specify the analytical form of the charge density and the Coulombic potential. This parameter was set to be OCTUPOLE which corresponds to L_{max} of 3.

The local density approximation (LDA) can be used to predict the structures and relative energies of covalent and ionic systems quite accurately. However, usually bond energies are overestimated while vibrational frequencies are underestimated than those obtained within other methods and experimental data. These problems with the LDA method can be corrected to large extent by using the so-called gradient-corrected (or non-local) functionals. However, extensive test calculations with local and non-local functionals yielded that in the case of SF_6 it is the LDA method with Perdew–Wang functional (PWC) that yield the results closer to available experimental data.

Table 1. Experimental and calculated properties of the SF_6 molecule.

Parameter	Unit	Present	Ref. [38]	Ref. [39][a]	Experiment
Binding energy[b]	eV	26.81	25.06	26.12	22.06 (20.12)
d(S—F)	Å	1.587	1.584	1.588	1.564[c]
ν_1 A_{1g}	cm^{-1}	723.5	–	718	772.269[d]
ν_2 E_g	cm^{-1}	625.5	–	622	641.608[d]
ν_3 F_{1u}	cm^{-1}	938.1	–	931	947.289[d]
ν_4 F_{1u}	cm^{-1}	567.2	–	562	614.589[d]
ν_5 F_{2g}	cm^{-1}	477.9	–	476	523.449[d]
ν_6 F_{2u}	cm^{-1}	315.7	–	312	348.428[d]

[a]PWC calculation. [b]$SF_6 \rightarrow S + 6F$. [c]Table 8 in [18], p. 280. [d]Table 7 in [18], p. 280.

We have therefore adopted this approach in all calculations performed for the purpose of the present study.

Vibrational spectra and Hessians were computed by finite differences of analytic first derivatives. This means that each atom in the system was displaced in each Cartesian direction. The results of Hessian evaluation have been used to compute thermodynamic properties of the molecules. Point group symmetry was used to reduce the total number of displacements. The vibrational analysis was performed at the final geometry. Hirshfeld partitioned charges were defined relative to the deformation density. Finally, the convergence criteria were established to be FINE both for the SCF density convergence (the density convergence threshold for SCF) and for the optimisation energy convergence (the threshold for energy convergence during geometry optimisation). The numerical values for these thresholds were 10^{-6} Ha and 10^{-5} Ha, respectively.

3. Results and discussion

3.1 Geometry optimisation

The accuracy of the data obtained in the course of the present study can be compared only in the case of the reference SF_6 molecule. There have been quite a number of electronic properties calculations for this system, and the predicted properties vary remarkably depending upon the methodology of the computation (see [38] for the discussion). Therefore, we decided to compare results yielded by our calculation with theoretical studies founded on DFT [38,39] that are available for the SF_6 molecule. The first and the most extensive work (however, without calculated vibrational frequencies) came from Tang and Callaway [38] who performed calculations for SF_6 in the local spin density (LSD) approximation. Delley [39] studied static deformations and vibrations of SF_6 with an applied strong static electric field; basic molecular properties in the absence of external electrostatic fields in local as well as gradient corrected approximations to DFT were obtained. To our knowledge, these are all numerical studies of the electronic structure of the SF_6 molecule based on the DFT methodology. Molecular properties of SF_6 are collected in Table 1.

It can be seen from Table 1 that our results obtained for the SF_6 molecule are in good agreement with those presented in [38,39]. The maximum deviation of calculated frequencies is at $49\,cm^{-1}$, which is less than 10% in comparison with experimental values. The LDA PWC approximation thus gives a fairly accurate description of the energy surface near the equilibrium conformation. Surprisingly enough, the gradient corrected functionals perform significantly worse for this molecule, except for the binding energy.

The equilibrium structures as obtained from optimisation of geometry of all studied molecules in their ground states are shown in Figure 1. The structures were optimised in imposed symmetry, relevant to each molecule (see the labels under the figure labels), in order to reduce the computational time whenever possible. The highest symmetry point group O_h is adopted by the SF_6 molecule, as well as by the SH_6 and SCl_6 ones. With the substitution of fluorine atoms with the hydrogen ones the symmetry is lowered, but symmetries of the $SF_{6-n}H_n$ ($n = 1,\ldots,5$) molecules are consistent with the correlation table of the O_h group. For molecules $SF_{6-n}H_n$ ($n = 2,3,4$) two possible non-equivalent conformations exist: the first one, denoted as (a), in which one of the hydrogen atoms is perpendicular to other hydrogen atom(s), and the second one, denoted as (b), in which all hydrogen atoms are in the same plane. Subsequent DMol[3] computations of other properties were performed at these final geometries.

Closer examination of structural data obtained shows that geometry of the $SF_{6-n}H_n$ ($n = 1,\ldots,6$) molecules resembles that of the SF_6 parent one. Because of the large amount of data collected detailed values of bond lengths and angles are available at http://www.icm.edu.pl/~jp/SF6_bonds_angles.pdf. For the purpose of the present study only principal trends are summarised. The relevant H–S–F angles are very close to 90° or 180°, respectively. The most deformed structure is that of SF_2H_4a with low, C_{2v} symmetry. The deviation from 180° is about 10°. The molecular distances between sulphur and fluorine atoms increase as the fluorine atoms are substituted by the

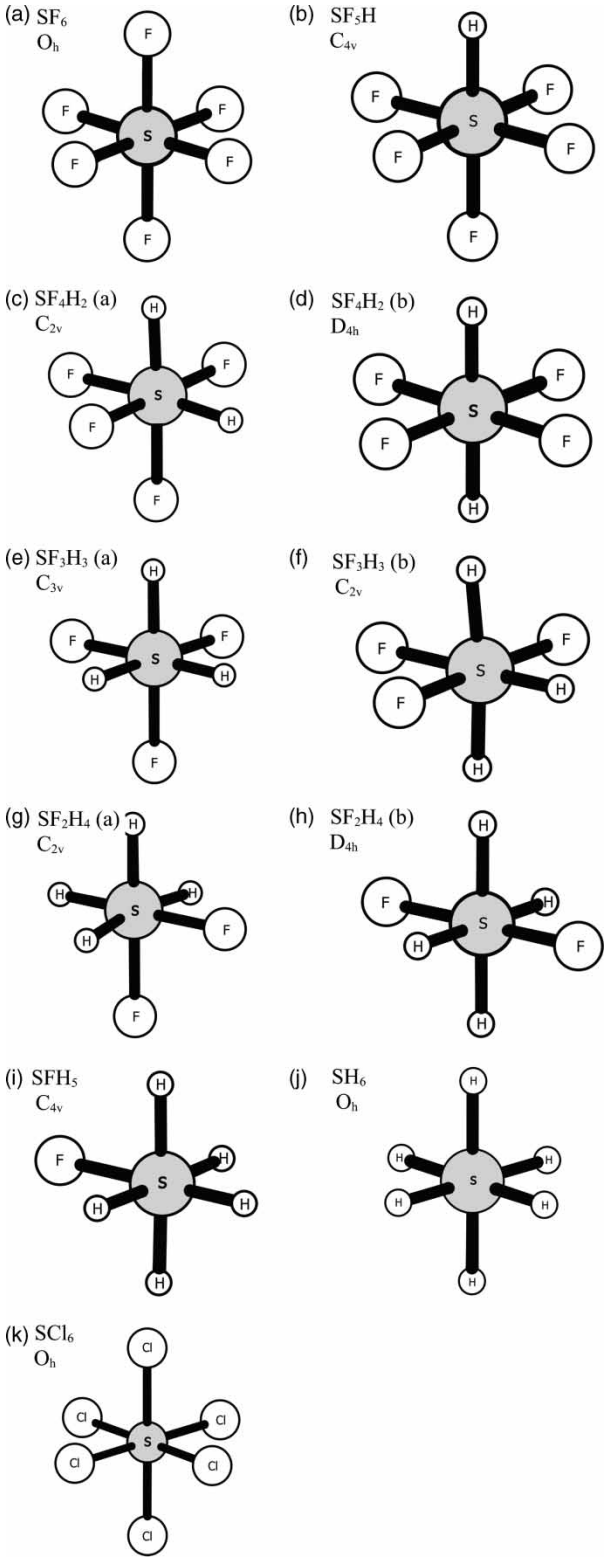

Figure 1. Equilibrium geometries of the $SF_{6-n}H_n$ ($n = 0, \ldots, 6$) series and SCl_6 in their ground states: (a) SF_6, O_h symmetry; (b) SF_5H, C_{4v} symmetry; (c) SF_4H_2a, C_{2v} symmetry; (d) SF_4H_2b, D_{4h} symmetry; (e) SF_3H_3a, C_{3v} symmetry; (f) SF_3H_3b, C_{2v} symmetry; (g) SF_2H_4a, C_{2v} symmetry; (h) SF_2H_4b, D_{4h} symmetry; (i) SFH_5, C_{4v} symmetry; (j) SH_6, O_h symmetry and (k) SCl_6, O_h symmetry.

hydrogen ones, and hydrogen–sulphur distances are smaller than the fluorine–sulphur ones. These trends are illustrated in Figure 2(a) and (b). It is worth to mention that in the case of SCl_6 the chlorine–sulphur distance is significantly larger and equals to 2.1461 Å.

The results obtained for binding energies for the $SF_{6-n}H_n$ ($n = 0, \ldots, 6$) series and SCl_6 are listed in Table 2. The SF_6 molecule has the highest binding energy as compared to the $SF_{6-n}H_n$ ($n = 1, \ldots, 6$) series. Interestingly enough, the SCl_6 and SH_6 molecules have similar values of binding energies. Since, the SF_6, SH_6 and SCl_6 molecules have octahedral symmetry, as well as the SF_4H_2b and SF_2H_4b have tetragonal symmetry, there are no static dipole moments in their case. The values of dipole moments obtained for the molecules under study are listed in Table 3, and its analysis is postponed to Section 3.3.

Closer examination of single particle eigenvalues (depicted in Figure 3) yields that with increasing number of the H atoms in the $SF_{6-n}H_n$ system the number of eigenstates is gradually diminishing, as there are less electrons. Symmetries of the orbitals are changing according to the symmetries of the given $SF_{6-n}H_n$ system (in order to keep the Figure 3 as readable as possible we decided to label eigenstates only for SF_6 and SH_6 molecules). Because of the same molecular symmetry of the SF_6 and SH_6 molecules molecular orbitals have the same symmetry in their case. However, there are fewer electrons in SH_6 than in SF_6, so only six first single particle eigenstates in three energetically lowest states with symmetries A_{1g}, T_{1u} and E_g are occupied.

3.2 Optical properties

Explicit values of the frequencies and intensities of the normal modes for all the $SF_{6-n}H_n$ ($n = 0, \ldots, 6$) molecules are listed in Tables 4 and 5, respectively, supplemented with data obtained for SCl_6. In Table 6, square of first derivatives of molecular dipole moments w.r.t. infrared active normal modes are shown.

The infrared absorption spectrum of SF_6 is composed of two bands. Only ν_3 and ν_4 modes with F_{1u} symmetry satisfy dipole selection rules and are allowed in absorption. Their maxima are located at 567.2 and 938.06 cm^{-1} with intensity 22.17 and 390.19 km/mol, respectively. Both of these normal modes are triple degenerate and correspond to the change of bond lengths and bond angles.

The frequencies of vibrations are expected to increase as hydrogen atoms are substituted for fluorine ones. This effect can be attributed to the extension of reduced masses of these molecules, as well as the decrease of intermolecular interactions (see Figure 2(a) and (b), as well as Table 2): binding energies are decreasing and bond lengths are increasing. As a consequence, with increasing n in $SF_{6-n}H_n$ ($n = 0, \ldots, 6$) spectra are shifted into higher

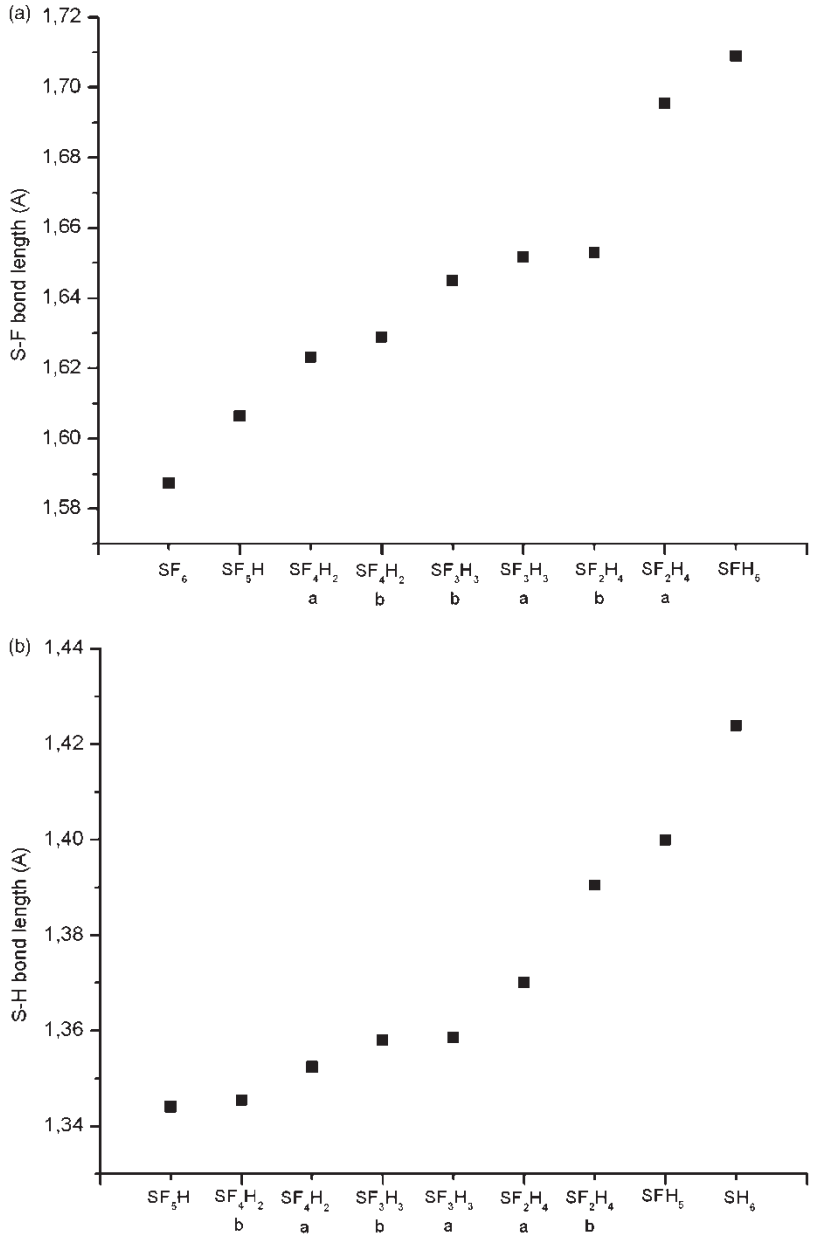

Figure 2. Interatomic distances in the $SF_{6-n}H_n$ ($n = 0, \ldots, 6$) series and SCl_6 (a) fluorine–sulphur distances and (b) hydrogen–sulphur distances.

energies. Variations in mass distribution and molecular geometries cause also alterations in symmetries of normal modes. The intensity of absorption for the fundamental vibrational transitions is given by:

$$A = B_{\mathrm{nw}} \cdot h \cdot \nu_{\mathrm{nw}} \cdot c^{-1} \cdot N_A,$$

where A is the integral coefficient of absorption (measure of absorption in band), ν_{nw} is the frequency of transition between n and w levels, and B_{nw} is the Einstein coefficient for induced emission, which can be expressed as:

$$B_{\mathrm{nw}} = \frac{8\pi^3}{3h^2} \cdot |\mu_{\mathrm{nw}}^2|,$$

in which μ_{nw} is the transition moment for n and w levels. For the fundamental transitions, this quantity is proportional to square of first derivatives of molecular dipole moments w.r.t. infrared active normal modes. As it is shown in Table 6, these values are increasing with the increasing rate of replacement of fluorine by hydrogen.

Table 2. Binding energy in eV and J.

Molecule	Symmetry	Binding energy	
		eV	J ($\times 10^{-18}$)
SF_6	O_h	26.810	4.295
SF_5H	C_{4v}	25.663	4.112
SF_4H_2a	C_{2v}	24.090	3.860
SF_4H_2b	D_{4h}	24.508	3.927
SF_3H_3a	C_{3v}	22.381	3.586
SF_3H_3b	C_{2v}	22.565	3.615
SF_2H_4a	C_{2v}	20.670	3.316
SF_2H_4b	D_{4h}	20.058	3.214
SFH_5	C_{4v}	18.165	2.910
SH_6	O_h	15.230	2.440
SCl_6	O_h	14.372	2.303

Table 3. Magnitudes of dipole moment vectors in Debye and C m.

Molecule	Symmetry	Dipole magnitude	
		Debye	C m ($\times 10^{-30}$)
SF_6	O_h	0.080	0.267
SF_5H	C_{4v}	1.752	5.844
SF_4H_2a	C_{2v}	2.659	8.871
SF_4H_2b	D_{4h}	0.001	0.003
SF_3H_3a	C_{3v}	3.634	12.122
SF_3H_3b	C_{2v}	2.151	7.175
SF_2H_4a	C_{2v}	3.392	11.314
SF_2H_4b	D_{4h}	0.067	0.223
SFH_5	C_{4v}	2.610	8.706
SH_6	O_h	0.039	0.131
SCl_6	O_h	0.042	0.141

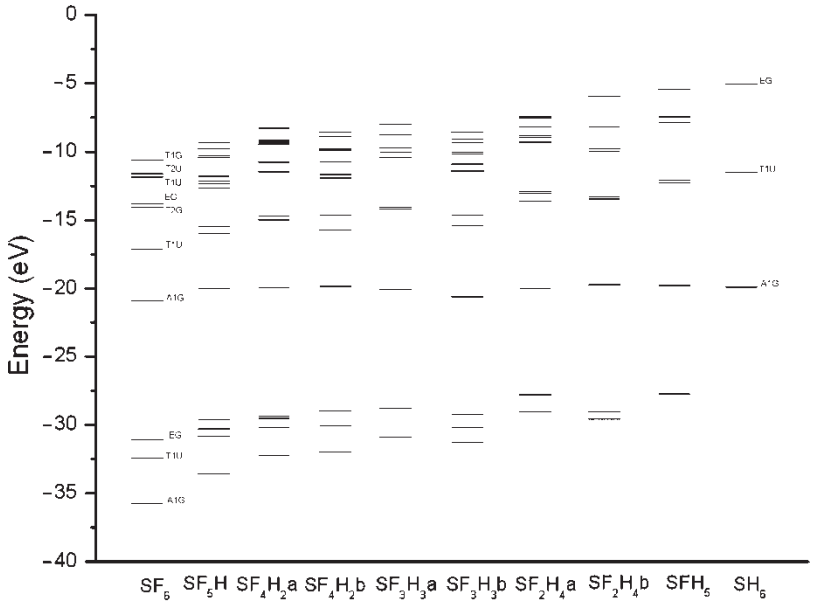

Figure 3. Single particle eigenvalues for the $SF_{6-n}H_n$ ($n = 0, \ldots, 6$) series. For readability only eigenstates for SF_6 and SH_6 molecules are labelled.

Table 4. Frequencies of normal modes in cm^{-1}.

Mode	SF_6	SF_5H	SF_4H_2a	SF_4H_2b	SF_3H_3a	SF_3H_3b	SF_2H_4a	SF_2H_4b	SFH_5	SH_6	SCl_6
7	315.6	296.3	325.8	276.2	367.2	346.9	337.7	430.8	630.4	1319.5	139.7
8	315.6	346.2	348.2	380.1	367.2	375.9	634.1	430.8	787.3	1319.5	139.7
9	315.6	346.2	399.4	380.1	486.3	422.0	675.0	611.7	787.3	1319.5	139.7
10	477.7	449.0	464.4	418.7	690.7	607.4	774.9	837.5	1112.5	1322.8	205.7
11	477.7	515.3	530.6	584.6	690.7	698.4	890.6	937.2	1220.5	1322.8	205.7
12	477.7	515.3	620.0	642.6	786.5	844.9	956.3	1119.8	1264.9	1322.8	205.7
13	567.0	572.6	718.4	649.4	866.8	941.8	1213.5	1119.8	1264.9	1329.3	230.7
14	567.0	606.5	809.6	860.2	1098.6	1134.9	1228.2	1299.7	1405.5	1329.3	230.7
15	567.0	659.2	875.7	860.2	1098.6	1159.4	1338.8	1423.6	1405.5	1329.3	230.7
16	625.0	832.1	1086.8	1195.5	1347.1	1262.4	1352.8	1423.6	1553.4	1909.2	253.9
17	625.0	902.6	1169.1	1195.5	1361.3	1280.3	1402.4	1651.4	2070.1	1909.2	263.2
18	722.9	902.6	1263.1	1253.2	1361.3	1449.0	2451.8	2174.4	2198.5	2014.5	263.2
19	937.4	1241.0	1391.9	1253.2	2575.2	2523.6	2484.5	2293.1	2198.5	2014.5	400.1
20	937.4	1241.0	2621.4	2649.1	2575.5	2540.9	2501.8	2293.1	2277.0	2014.5	400.1
21	937.4	2707.1	2636.2	2725.0	2575.5	2592.0	2505.1	2354.9	2438.2	2173.2	400.1

Table 5. Intensities of normal modes in km mol^{-1}.

Mode	SF_6	SF_5H	SF_4H_2a	SF_4H_2b	SF_3H_3a	SF_3H_3b	SF_2H_4a	SF_2H_4b	SFH_5	SH_6	SCl_6
7	0	0	1.5	0	0.9	0.8	0.3	20.5	168	0	0
8	0	1.3	0	5.1	0.9	3.8	171.2	20.5	2.4	0	0
9	0	1.3	7.9	5.1	4.5	26.7	186.8	0	2.4	0	0
10	0	0	3.4	0	156.1	13.1	0	361.6	0	0	0
11	0	8.7	8.4	0	156.1	191.5	5	0	30.2	0	0
12	0	8.7	10.2	90.3	188.3	389.1	27.2	0	6.9	0	0
13	22.2	19.1	168.8	0	0	33.1	12.6	0	6.9	49.6	1.3
14	22.2	0	192.2	417.7	20.7	0.1	12.8	11.7	32.2	49.6	1.3
15	22.2	14.9	395.6	417.7	20.7	0	1	40.3	32.2	49.6	1.3
16	0	189.4	25.9	0	5.6	9.1	4.5	40.3	0	0	0
17	0	407.7	0	0	1.7	1.1	0	0	0	0	0
18	0	407.7	0.3	0.5	1.7	2.6	4.6	0	357.3	678.2	0
19	390.2	0.1	1.7	0.5	40.6	33.5	58.5	284.2	357.3	678.2	116.7
20	390.2	0.1	15.1	0	26.4	24.1	44.3	284.2	0	678.2	116.7
21	390.2	0.2	13.6	0.05	26.4	17.6	82.1	0	99.5	0	116.7

Table 6. Square of first derivatives of molecular dipole moments w.r.t. infrared active normal modes in a.u.

Mode	SF_6	SF_5H	SF_4H_2a	SF_4H_2b	SF_3H_3a	SF_3H_3b	SF_2H_4a	SF_2H_4b	SFH_5	SH_6	SCl_6
7	0	0	0	0	0.001	0.001	0	0.021	0.17	0	0
8	0	0.001	0	0.005	0.001	0.004	0.175	0.021	0.003	0	0
9	0	0.001	0.01	0.005	0.005	0.027	0.191	0	0.003	0	0
10	0	0	0	0	0.159	0.014	0	0.369	0	0	0
11	0	0.009	0.01	0	0.159	0.195	0.005	0	0.03	0	0
12	0	0.009	0.01	0.092	0.192	0.397	0.028	0	0.007	0	0
13	0.02	0.019	0.17	0	0	0.034	0.013	0	0.007	0.05	0.001
14	0.02	0	0.2	0.427	0.021	0	0.013	0.012	0.033	0.05	0.001
15	0.02	0.015	0.4	0.427	0.021	0	0.001	0.041	0.033	0.05	0.001
16	0	0.193	0.03	0	0.006	0.009	0.005	0.041	0	0	0
17	0	0.416	0	0	0.002	0.001	0	0	0	0	0
18	0	0.416	0	0	0.002	0.003	0.005	0	0.364	0.69	0
19	0.4	0	0	0	0.041	0.031	0.06	0.29	0.364	0.69	0.119
20	0.4	0	0.02	0	0.027	0.028	0.045	0.29	0	0.69	0.119
21	0.4	0	0.01	0	0.027	0.018	0.084	0	0.1	0	0.119

Molecules SCl_6 and SH_6 are again quite similar to SF_6. As they adopt O_h point group symmetry, the infrared spectra are analogous to this of SF_6. The difference is in the frequencies of normal modes and intensities of their absorption. SCl_6, as a heavier molecule, has lower vibrational transition intensity as well as lower frequencies of normal modes. In contrast to this, SH_6 has much higher vibrational transition intensity and higher frequencies of normal modes. This means that SH_6 absorbs even more radiation than SF_6, but in the range of higher frequencies. SH_6 has also nearly two times lower binding energy than SF_6 and, as such, is less stable.

It is also worth to mention that strongest absorption band of SF_6 at $\sim 940\,cm^{-1}$ is located in the atmospheric window mentioned in Section 1, and no other molecule studied here has so strong absorption band in this frequency region as SF_6 has.

Table 7. Charges partitioned by Hirshfeld method.

		Charges		
Molecule	Symmetry	S	F	H/Cl
SF_6	O_h	0.5801	−0.0967	−
SF_5H	C_{4v}	0.5013	−0.1148	0.0729
SF_4H_2a	C_{2v}	0.4224	−0.1333	0.0553
SF_4H_2b	D_{4h}	0.4249	−0.1419	0.0714
SF_3H_3a	C_{3v}	0.3396	−0.1591	0.0459
SF_3H_3b	C_{2v}	0.3459	−0.1643	0.0490
SF_2H_4a	C_{2v}	0.2613	−0.2078	0.0386
SF_2H_4b	D_{4h}	0.2776	−0.1619	0.0116
SFH_5	C_{4v}	0.1917	−0.2248	0.0066
SH_6	O_h	0.1361	−	−0.0227
SCl_6	O_h	0.3411	−	−0.0568

3.3 Charge distribution and dipole moments

Charge partitioning as obtained from Hirshfeld method for all the $SF_{6-n}H_n$ ($n = 0,\ldots,6$) molecules and the SCl_6 one is listed in Table 7. These values are normalised to single atoms, so one should bear in mind that for given n in $SF_{6-n}H_n$ $q_S = (6-n)q_F + nq_H$. Hirshfeld analysis for SF_6 indicates positive charge on the sulphur atom and small negative charges on the fluorine atoms. Negative charges on the fluorine atoms increase while positive charge on the sulphur atom decreases as fluorine atoms are gradually substituted with the hydrogen atoms. Although not included here, the results of Mulliken analysis are consistent with the results of Hirshfeld one.

The dipole moment of a molecule is determined by the charges and the induced dipoles on the constituent atoms. Because of symmetric charge distribution, there are no static dipole moments in molecules: SF_6, SF_4H_2b, SF_2H_4b, SH_6 and SCl_6. The SF_5H has almost two times smaller magnitude of dipole moment than SFH_5, although charges on constituent atoms are larger in SF_5H than in SFH_5, and both molecules have the same symmetry. One can assume that for SFH_5 the charge and induced dipole contributions have the same polarity that account for its large dipole moment, in contrast to SF_5H. In case of the SF_3H_3a and b molecules the large difference in dipole moments is caused by different symmetry of charge distribution.

3.4 Thermodynamical properties

Basic thermodynamic properties such as total entropy, vibrational entropy, free energy, heat capacity and zero point vibrational energy (ZPVE) have been also calculated for the $SF_{6-n}H_n$ ($n = 0,\ldots,6$) and SCl_6 molecules. The results are presented in Table 8. Additionally, entropy as a function of temperature for all the molecules studied here is depicted in Figure 4. Values of heat capacity decrease with molecular mass reduction. As the heat capacity is defined as the amount of heat required to change the temperature of a substance by 1°, larger molecules will need more heat than smaller ones. This suggests that insulating properties of SCl_6 are the best of all the molecules studied here, in particular better than these of SF_6. The industrial usage of SF_6 instead of SCl_6 is due to greater stability of SF_6 than SCl_6 (bonding energy for SF_6 is twice higher than that for SCl_6). Total and vibrational entropy decreases as fluorine atoms are substituted with hydrogen ones. On the other hand, the free energy and zero point vibrational entropy show opposite tendency. This behaviour is in good relation to changes in molecular mass of studied compounds.

4. Conclusions

In the present study the series of the $SF_{6-n}H_n$ ($n = 0,\ldots,6$) molecules have been examined for the first time. Molecular constants such as equilibrium bond distances, binding energies, vibrational frequencies, charge distributions partitioned by Hirshfeld method, dipole moments, as well as thermodynamic properties have been determined and analysed.

The results of IR spectra simulations confirm that it is fluorine atoms that play crucial role in greenhouse effect of SF_6. For other molecules with octahedral symmetry, such as SH_6 and SCl_6, their absorption bands are outside the atmospheric window. On the other hand, for the $SF_{6-n}H_n$ ($n = 1,\ldots,5$) molecules with lower symmetries, there are more absorptions bands with reduced intensities as compared to SF_6.

Because of inherent approximations in DFT, computational methods based on this approach are not expected to yield very accurate values of molecular constants, as wave function based *ab initio* methods do. Rather, due to their efficiency and robustness DFT-based methods constitute valuable tool in predicting general trends across a wide range of compounds. Therefore, the present study can be regarded as the first step toward more detailed

Table 8. Thermodynamic properties.

Molecule	Symmetry	Total entropy (cal mol^{-1} K^{-1})	Vibrational entropy (cal mol^{-1} K^{-1})	ZPVE (kcal mol^{-1})	Free energy (kcal mol^{-1})	Heat capacity (cal mol^{-1} K^{-1})
SF_6	O_h	77.235	9.128	12.682	−18.776	24.175
SF_5H	C_{4v}	74.798	7.662	17.349	−18.355	21.553
SF_4H_2a	C_{2v}	71.896	5.977	21.816	−17.829	18.883
SF_4H_2b	D_{4h}	72.350	6.239	21.906	−17.928	18.933
SF_3H_3a	C_{3v}	68.412	4.780	26.870	−17.165	16.156
SF_3H_3b	C_{2v}	68.879	4.337	25.992	−17.262	16.249
SF_2H_4a	C_{2v}	65.210	2.576	29.664	−16.462	13.770
SF_2H_4b	D_{4h}	64.384	2.624	29.165	−16.259	13.735
SFH_5	C_{4v}	60.170	1.800	32.541	−15.331	11.263
SH_6	O_h	54.932	0.231	34.238	−13.948	9.253
SCl_6	O_h	101.464	28.160	5.302	−23.158	34.214

ZPVE: zero point vibrational energy.

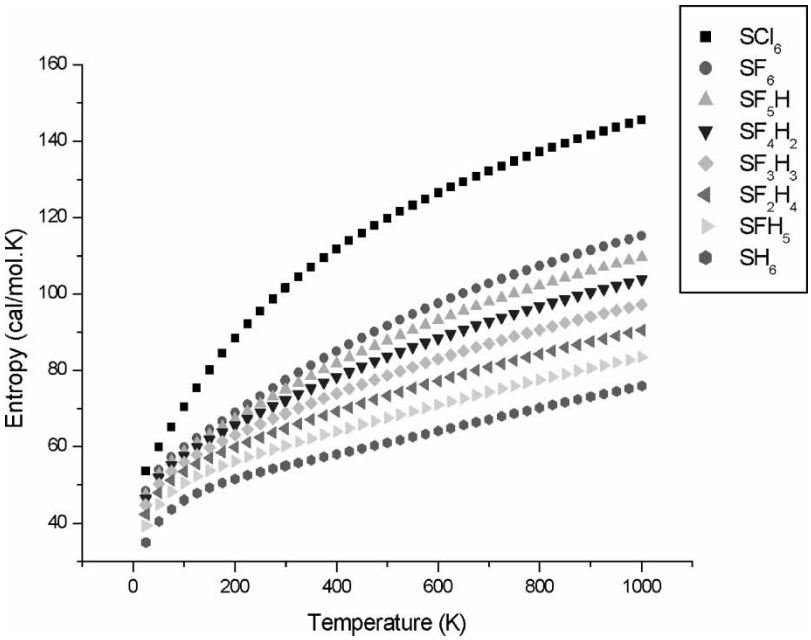

Figure 4. Entropy as a function of temperature for the $SF_{6-n}H_n$ ($n = 0, \ldots, 6$) molecules and SCl_6.

examination of the series of $SF_{6-n}H_n$ ($n = 0, \ldots, 6$) molecules. Further research can cover following areas:

(1) formation of metastable negative ions;
(2) reaction paths with OH radicals and
(3) investigation of excited states.

These topics are outside the scope of the present study, but the need for further *ab initio* calculations for these systems is therefore obvious.

Acknowledgements

The authors are indebted to Dr Paweł M. Masiak, Institute of Physics, Polish Academy of Sciences, for many valuable discussions, and to Dr Carsten Menke, Accelrys, Inc., for his technical assistance with the DMol^3 code.

References

[1] *IEE Colloquium on An Update in SF6 and Vacuum Switchgear at Distribution Levels*, (Digest No. 1996/185), IEE, London (1996).
[2] D.C. Frost, C.A. McDowell, J.S. Sandhu, and D.A. Vroom, *Photoelectron spectrum of sulfur hexafluoride at 584 Å*, J. Chem. Phys. 46 (1967), pp. 2008–2009.
[3] B.M. Addison Jones, K.H. Tan, G.M. Bancroft, and F. Cerrina, *A comparison of shape resonant behavior in the inner-shell photo-absorption and valence-level photoelectron spectra of sulfur hexafluoride, sulfur chloride fluoride and selenium hexafluoride (SF_6, SF_5Cl and SeF_6)*, Chem. Phys. Lett. 129 (1986), pp. 468–474.
[4] B.M. Addison Jones, K.H. Tan, B.W. Yates, J.N. Cutler, G.M. Bancroft, and J.S. Tse, *A comparison of valence level photoelectron cross sections for SF_6, SeF_6 and 'F_6' from 21 eV to 100 eV photon energy*, J. Electron Spectrosc. Relat. Phenon. 48 (1989), pp. 155–178.
[5] V.H. Dibeler and J.A. Walker, *Photoionization efficiency curve for SF6 in the wavelength region 1050 to 600 Å*, J. Chem. Phys. 44 (1966), pp. 4405–4406.
[6] R.N. Compton, R.H. Huebner, P.W. Reinhardt, and L.G. Christophroou, *Threshold electron impact excitation of atoms and molecules: Detection of triplet and temporary negative ion states*, J. Chem. Phys. 48 (1968), pp. 901–909.
[7] D.M.P. Holland, D.A. Shaw, A. Hopkirk, M.A. MacDonald, and S.M. McSweeney, *A study of the absolute photoabsorption cross section and the photoionization quantum efficiency of sulfur hexafluoride from the ionization threshold to 420 Å*, J. Phys. B 25 (1992), pp. 4823–4834.
[8] T.A. Ferret, D.W. Lindle, P.A. Heimann, M.N. Piancastelli, P.H. Kobrin, H.G. Kerkhoff, U. Becker, W.D. Brewer, and D.A. Shirley, *Shape-resonant and many-electron effects in the S 2p photoionization of sulfur hexafluoride*, J. Chem. Phys. 89 (1988), pp. 4726–4736.
[9] R.E. LaVilla, *Sulfur K and L and fluorine K X-ray emission and absorption spectra of gaseous sulfur hexafluroide*, J. Chem. Phys. 57 (1972), pp. 809–909.
[10] D. Blechschmidt, R. Haensel, E.E. Koch, U. Nielsen, and T. Sagawa, *Optical spectra of gaseous and solid sulfur hexafluoride in the extreme ultraviolet and soft X-ray region*, Chem. Phys. Lett. 14 (1972), pp. 33–36.
[11] J.L. Dehmer, *Evidence of effective potential barriers in the X-ray absorption spectra of molecules*, J. Chem. Phys. 56 (1972), pp. 4496–4504.
[12] T. Sakae, S. Sumiyoshi, E. Murakami, Y. Matsumoto, K. Ishibashi, and A. Katase, *Scattering of electrons by methane, carbon tetrafluoride and sulfur hexafluoride in the 75–700 eV range*, J. Phys. B 22 (1989), pp. 1395–1409.
[13] A.P. Hitchcock, E. Brion, and M.J. van der Wiel, *Ionic fragmentation of sulfur hexafluoride ionized in the sulfur 2p shell*, J. Phys. B 11 (1978), pp. 3245–3261.
[14] A.P. Hitchcock and C.E. Brion, *Inner shell excitation of sulfur hexafluoride by 2.5 keV electron impact*, Chem. Phys. 33 (1978), pp. 55–64.
[15] K.H. Sze and C.E. Brion, *Inner-shell and valence-shell electronic excitation of sulfur hexafluoride, selenium hexafluoride, and tellurium hexafluoride by high energy electron impact: An investigation of potential barrier effects*, Chem. Phys. 140 (1990), pp. 439–472.
[16] J.F. Ying, C.P. Mathers, and K.T. Leung, *Momentum-transfer dependence of sulfur 2p excitations in sulfur hexafluoride by*

angle-resolved electron-energy-loss spectroscopy, Phys. Rev. A 47 (1993), pp. R5–R8.
[17] K. Kim, R.S. McDowell, and W.T. King, *Integrated infrared intensities and transition moments in SF6*, J. Chem. Phys. 73 (1980), pp. 36–41.
[18] L.G. Christophorou and J.K. Olthoff, *Electron interactions with SF_6*, J. Phys. Chem. Ref. Data 29 (2000), pp. 267–330.
[19] A. Chutjian, A. Garscadden, and J.M. Wadehra, *Electron attachment to molecules at low electron energies*, Phys. Rep. 264 (1996), pp. 393–470.
[20] R. Morrow, *Theory of electrical corona in SF_6*, Nucl. Instr. Meth. Phys. Res. A 382 (1996), pp. 57–65.
[21] P.-T. Howe, A. Kortyna, M. Darrach, and A. Chutjian, *Low-energy electron attachment to SF_6 at sub-meV resolution using a tunable laser photoelectron method*, Phys. Rev. A 64 (2001), 042706.
[22] IPCC Working Group 1 (WG1) *Changes in Atmospheric Constituents and in Radiative Forcing, in IPCC Fourth Assessment Report (AR4)*, available at http://ipccwg1.ucar.edu/wg1/wg1-report.html (2007)
[23] M. Ko, N. Sze, W.-C. Wang, G. Shia, A. Goldman, F. Murcray, D. Murcray, and C. Rinsland, *Atmospheric sulfur hexafluoride: Sources, sinks and greenhouse warming*, J. Geophys. Res. 98(D6) (1993), pp. 10499–10507.
[24] R. Morris, T. Miller, A. Viggiano, J. Paulson, S. Solomon, and G. Reid, *Effects of electron and ion reactions on atmospheric lifetimes of fully fluorinated compounds*, J. Geophys. Res. 100(D1) (1995), pp. 1287–1294.
[25] L. Geller, J. Elkins, J. Lobert, A. Clarke, D. Hurst, J. Butler, and R. Myers, *Tropospheric SF_6: Observed latitudinal distribution and trends, derived emissions and interhemispheric exchange time*, Geophys. Res. Lett. 24 (1997), pp. 675–678.
[26] W.-T. Tsai, *The decomposition products of sulfur hexafluoride (SF6): Reviews of environmental and health risk analysis*, J. Fluorine Chem. 128 (2007), pp. 1345–1352.
[27] *Kyoto Protocol to the United Nations Framework Convention on Climate Change*, available at http://unfccc.int/resource/docs/convkp/kpeng.pdf
[28] W.T. Sturges, T.J. Wallington, M.D. Hurley, K.P. Shine, K. Sihra, A. Engel, D.E. Oram, S.A. Penkett, R. Mulvaney, and C.A.M. Brenninkmeijer, *A potent greenhouse gas identified in the atmosphere: SF5CF3*, Science 289 (2000), pp. 611–613.
[29] P. Masiak and A.L. Sobolewski, *Theoretical study of the photophysics of SF5CF3*, Chem. Phys. 313 (2005), pp. 169–176.
[30] *PFC, HFC, SF_6 Emissions from Semiconductor Manufacturing, in Good Practice Guidance and Uncertainty Management in National Greenhouse Gas Inventories*, Available at http://www.ipcc-nggip.iges.or.jp/public/gp/english/ p. 3.69
[31] A. Sekiya, M. Yamabe, K. Tokuhashi, Y. Hibino, R. Imasu, and H. Okamoto, *Evaluation and selection of CFC alternatives*, in *Fluorine and the Environment: Atmospheric Chemistry, Emissions & Lithosphere* (*Advances in Fluorine Science, Vol. 1*), A. Tressaud, ed., Elsevier Science, Amsterdam, 2006.
[32] P. Hohenberg and W. Kohn, *Inhomogeneous electron gas*, Phys. Rev. 136 (1964), pp. B864–B871.
[33] W. Kohn and L.J. Sham, *Self-consistent equations including exchange and correlation effects*, Phys. Rev. 140 (1965), pp. A1133–A1138.
[34] J. Piechota and M. Suffczynski, *Electronic structure of the CoO molecule*, Phys. Rev. A 48 (1993), pp. 2679–2685.
[35] J. Piechota and M. Suffczynski, *Density functional study of the diatomic first row transition metal oxides*, Z. Phys. Chem. 200 (1997), pp. 39–49.
[36] B. Delley, *An all-electron numerical method for solving the local density functional for polyatomic molecules*, J. Chem. Phys. 92 (1990), pp. 508–517.
[37] B. Delley, *From molecules to solids with the $DMol^3$ approach*, J. Chem. Phys. 113 (2000), pp. 7756–7764.
[38] R. Tang and J. Callaway, *Electronic structure of SF_6*, J. Chem. Phys. 84 (1986), pp. 6854–6860.
[39] B. Delley, *Vibrations and dissociation of molecules in strong electric fields: N_2, NaCl, H_2O and SF_6*, J. Mol. Struct. (Theochem.) 434 (1998), pp. 229–237.